Grain Boundary Migration in Polycrystalline Graphene

Dana Zöllner[1], Jules Dake[2], Carl E. Krill III[2], Simon Kurasch[3], Ute Kaiser[3]
[1]Institute for Experimental Physics, Otto von Guericke University Magdeburg
[2]Institute of Micro and Nanomaterials, Ulm University
[3]Electron Microscopy Group, Ulm University

Introduction. It is well-known that most materials properties, like yield or fracture strength, depend strongly on the microstructure of a polycrystalline solid, in particular, on its average grain size, which changes, e.g, due to thermal processing with time leading to a coarsening of the grain structure. When attempting to investigate the underlying mechanisms of grain growth, one is faced with a profound problem: namely, the 3D nature of polycrystalline bulk materials. In such specimens, current characterization techniques lack the spatial and temporal resolution to capture the kinetics of grain boundary migration at the atomic level.
However, these technical limitations can be overcome by investigating a 2D material like polycrystalline graphene–simultaneously stimulated and observed by electron bombardment in an aberration-corrected high-resolution transmission electron microscope.

Problem Definition & Objectives

In the present study we analyze the migration of grain boundaries in polycrystalline graphene by the capillary fluctuation method on the atomic scale. Hence, **microscopic fluctuations** are evaluated to calculate the stiffness and the associated mobility of graphene grain boundaries (**macroscopic materials parameters**). The results are compared with Monte Carlo simulations, which are used to fill the gab between experiments and analytical descriptions explaining, e.g., deviations.
This work has been performed as part of a research stay at the Institute of Micro and Nanomaterials at Ulm University.

Cooperation

We would like to thank Peter Streitenberger, Albrecht Bertram and Matthias Kunik from the GKMM for helpful discussions.
In addition, we acknowledge the German Science Foundation (DFG) for financial support through project ZO 280/2 and through the SALVE II project.

Experimental Observations

In general, the lattice structure of graphene consists of hexagonal carbon rings with a carbon-carbon bond length of a = 0.142 nm. Then again, in polycrystalline graphene (Fig. 1) two adjacent grains are always separated by tilt grain boundaries, which consist of energetically optimal pairs of pentagonal-heptagonal carbon rings.

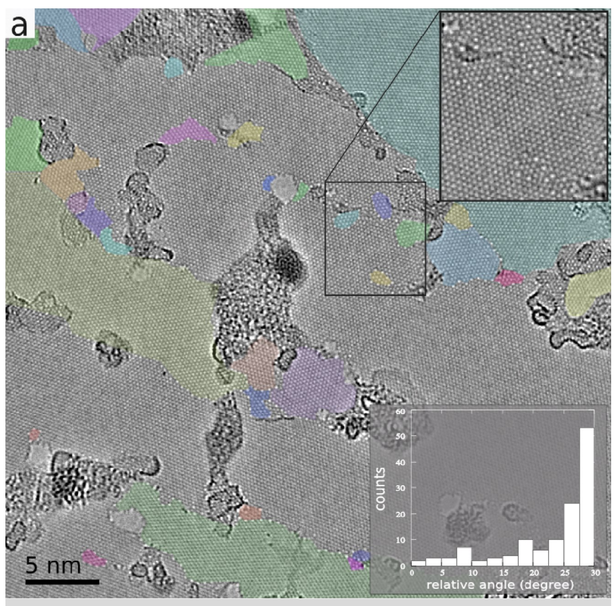

Figure 1. Graphene sample (see [1]).

Experiments of polycrystalline graphene were done in an aberration-corrected HR-TEM operated at 80 kV. The extraction voltage of the field emission source was set to a reduced value of 2 kV in order to minimize the energy spread of the electron beam, and the spherical aberration was set to 20 µm. Under these conditions, atoms appear dark (cf. Figs. 1 and 2).
Simultaneously, the energy of the imaging electrons stimulates individual bond rotations in the grain boundary core regions resulting in **morphological changes that can be followed in-situ, atom-by-atom**. The grain boundaries show a migration behavior analogously to grain growth, where only in presence of significant boundary curvatures a migration in a preferential direction can be observed [1].

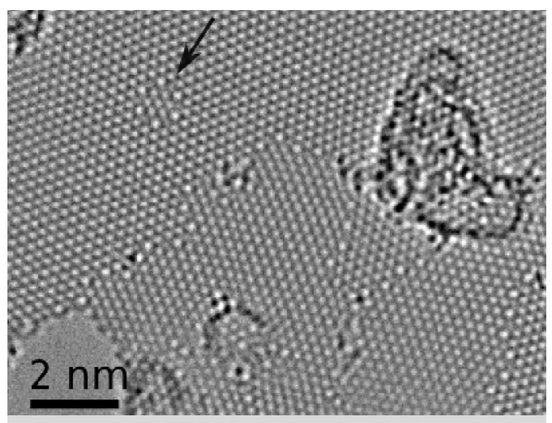

Figure 2. HRTEM image of grain boundaries and flower-like grain (arrow) [1].

Capillary Fluctuations

The capillary fluctuation method analyses the mean-square amplitude of capillary fluctuations. The interface height $h(x,t)$ is a function of location x and time t. In particular, the grain boundary fluctuations can be analyzed by calculating the time-dependent height-height correlation function (see [2, 3])

$$g(\mathrm{d}x,\mathrm{d}t)=\langle \Delta h(x,t)\cdot\Delta h(x+\mathrm{d}x,t+\mathrm{d}t)\rangle \qquad (1)$$

$\Delta h(x,t)=h(x,t)-\langle h(x)\rangle_t$ represents the position of the interface compared to the time-average position.

Hence, the static height-height correlation $g_s(\mathrm{d}x)$ follows from Fourier transformations to

$$g_s(\mathrm{d}x)=\frac{k_BT}{2\Gamma}\cdot\xi\cdot\exp(-\mathrm{d}x/\xi) \qquad (2)$$

where, in particular, the correlation length ξ has been introduced. The parameter k_BT describes the activation energy and Γ is the **grain boundary stiffness**.

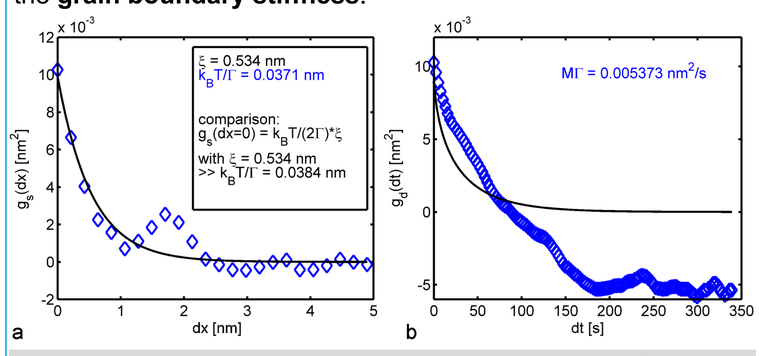

Figure 3. Experimental grain boundary of length $L = 4$ nm: a – static height correlation; b – dynamic height correlation.

On the other hand, the time-dependent correlation yields also the dynamic height-height correlation as

$$g_d(\mathrm{d}t)=\frac{k_BT}{2\Gamma}\xi\cdot\mathrm{erfc}\left(\xi^{-1}\cdot(M\Gamma\,\mathrm{d}t)^{1/2}\right) \qquad (3)$$

with the complementary error function $\mathrm{erfc}(\mathrm{d}t)$ and M describing the **grain boundary mobility**.

While height correlations of the long ($L >> 4$ nm) simulated grain boundary [4] are in perfect agreement with the analytic description according to Eqs. (2) and (3) (see Fig. 4), it can be seen in Fig. 3 that there are clear deviations between experiment and theory due to the short boundary length.

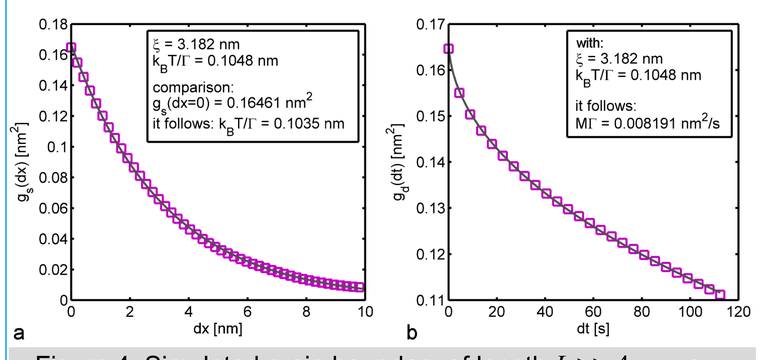

Figure 4. Simulated grain boundary of length $L >> 4$ nm: a – static height correlation; b – dynamic height correlation.

Flower Defect Analysis

The question arises, how trustworthy these values are, and at least for the product of mobility and stiffness $M\Gamma$ there is a second completely independent method for calculation.

Generally, the growth of grains during curvature driven annealing is done by migration of grain boundaries to the center of their curvature with a velocity of

$$v=-M\Gamma\cdot\kappa \qquad (4)$$

with κ as the sum over all main curvatures of the grain boundary segment. This yields for any closed plane curve

$$A=-2\pi\cdot M\Gamma\cdot t+A_0 \qquad (5)$$

Eq. (5) holds independent of the shape of the grain!

In particular, for the small flower-like grain in Fig. 2 the loss of area versus time in shown in Fig. 5, where it can be seen that A is indeed proportional to t.

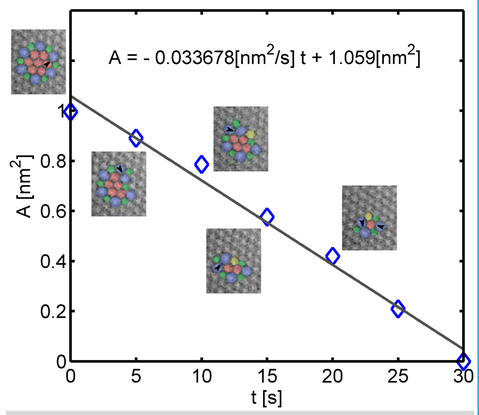

Figure 5. Shrinking flower defect.

This is quite astonishing considering that the above considerations of curvature driven grain growth, Eqs. (4) and (5), are mesoscopic contemplations, whereas in the experiment we are observing the grain boundary migration on an atomic level. The initial grain size is only 1 nm²!
Applying Eq. (5) to the shrinking kinetics the slope in Fig. 5 yields $M\Gamma = 5.360\cdot10^{-21}\,\mathrm{m^2/s}$. This is in **fantastic agreement** with the value obtained from the fluctuations of the flat grain boundary with $M\Gamma = 5.373\cdot10^{-21}\,\mathrm{m^2/s}$.

A comparison of the experimental kinetics with a Potts model simulation according to [4] is shown in Figure 6. Despite the fantastic overall agreement, this shows in an impressive way the influence of statistical fluctuations on the migration kinetics.

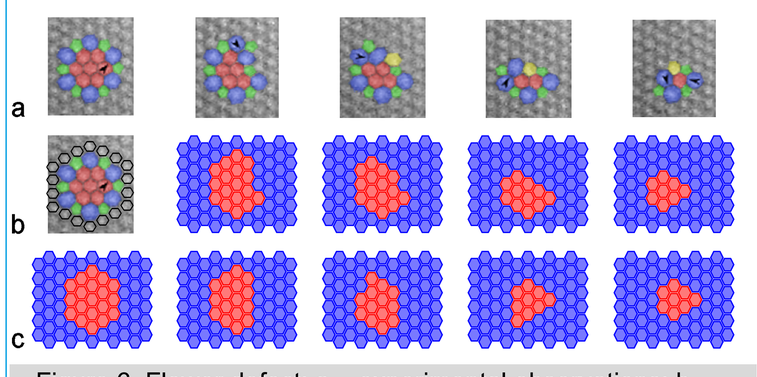

Figure 6. Flower defect: a – experimental observations; b – mapping to simulation lattice; c – simulation result.

Discussion and Conclusions

All in all, we have shown that the migration of individual grain boundaries in polycrystalline graphene–simultaneously stimulated and observed by electron bombardment in an aberration-corrected high-resolution transmission electron microscope–can be analyzed with the capillary fluctuation method yielding values for the boundary stiffness and the associated boundary mobility. The resulting product of stiffness and mobility is in very good agreement with the value obtained from an analysis of the shrinking kinetics of a small hexagonal graphene grain (flower defect).
In addition, Potts model simulations have been used to fill the gap between the analytic description in the framework of the capillary fluctuation method, Eqs. (1)-(3), and the experimental data. It has been found that the deviations are a size effect due to the very limited length of the observed grain boundary with a length of only approximately 4 nm. If it were possible to observe and analyze longer boundaries (preferably over longer time spans) the disagreement should vanish.

References

[1] S. Kurasch, J. Kotakoski, O. Lehtinen, V. Skákalová, J. Smet, C.E. Krill III, A.V. Krasheninnikov, U. Kaiser: Nano Lett. 12 (2012) 3168.

[2] T.O.E. Skinner, D.G.A.L. Aarts, R.P.A. Dullens: Phys. Rev. Lett. 105 (2010) 168301.

[3] D. Zöllner, J. Dake, C.E. Krill III: submitted to Scripta Mater.

[4] D. Zöllner, J. Dake, C.E. Krill III: Praktische Metallographie Sonderband 45, DGM INVENTUM (2013) 247.